Article:
Nelson, S., Geddes, D.A. orcid.org/0000-0001-6372-2551, Kearney, S.A. et al. (5 more authors) (2023) Hydrate assemblage stability of calcium sulfoaluminate-belite cements with varying sulfate content. Construction and Building Materials, 383. 131358. ISSN: 0950-0618

https://doi.org/10.1016/j.conbuildmat.2023.131358

Construction and Building Materials 383 (2023) 131358

Contents lists available at ScienceDirect

Construction and Building Materials

journal homepage: www.elsevier.com/locate/conbuildmat

Hydrate assemblage stability of calcium sulfoaluminate-belite cements with varying sulfate content

Shaun Nelson [a], Daniel A. Geddes [a], Sarah A. Kearney [a], Sally Cockburn [b], Martin Hayes [b], Michael J. Angus [b], Gavin Cann [b], John L. Provis [a,*]

[a] Department of Materials Science & Engineering, University of Sheffield, Sheffield S1 3JD, UK
[b] National Nuclear Laboratory, Havelock Road, Derwent Howe, Workington, Cumbria CA14 3YQ, UK

ARTICLE INFO

Keywords:
Calcium sulfoaluminate
Belite
Sulfate
Phase assemblage
Stability
Nuclear waste immobilisation

ABSTRACT

To assess the feasibility of employing calcium sulfoaluminate (CSA)-belite cements for radioactive waste encapsulation purposes, a series of 40 mixes were conducted on a 3-litre scale. This series of tests incorporated two commercially available CSA-belite clinkers, gypsum or anhydrite addition at 15, 25 or 35 wt%, a water to solids ratio of 0.5, 0.6 or 0.7, and a high or low mixing shear regime. CSA clinkers chosen contain predominantly ye'elimite, with some belite, and a small quantity of calcium sulfate as anhydrite. This paper outlines the effect of these parameters upon the phase composition and structure of these CSA samples tested at 7, 28, and 90 days. The development of the hydrate assemblage was monitored in order to assess the suitability of these grouts for use in encapsulation processes. The trends in phase development and evolution are consistent across both clinkers tested. The levels of ettringite formed as a hydration product are dependent upon the levels of calcium sulfate addition and the availability of water, with ettringite production evident, though at a decreasing rate, from between 7 and 90 days. Throughout the entire catalogue of mixes, no ettringite decomposition was detected. The majority of belite within both clinkers appears to remain unreacted, with a small increase in mixes producing less ettringite. Simulations also show similar phase assemblages to those encountered experimentally, with little phase development after 90 days.

1. Introduction

Calcium sulfoaluminate cement (CSA) is being considered by the UK nuclear industry as a potential future encapsulant for radioactive waste [1]. CSA has the potential to improve encapsulation performance and help secure a supply of cementitious material for long term future use, offering several potential key advantages such as: enhanced chemical resistance, an early age pore solution pH below 12, high water retention, and lower associated CO_2 emissions [1–4]. CSA is being developed as a low CO_2 alternative cement for applications requiring rapid strength development and high dimensional stability with shrinkage compensation, and has seen successful deployment in highway repair and runway paving [5,6]. It has also been used extensively in China since the 1970′s, where it is referred to as TCS or 'third cement series', with high alumina cement and Portland cement (PC) accounting for the second and first series respectively [4,7,8]. Whilst having shown promise in both large-scale projects and laboratory testing, CSA is a relatively new cement in comparison to PC and does not have nearly the same wealth of past experience associated with it. The UK nuclear industry has long relied upon PC based systems, combined with supplementary cementitious materials (SCMs), to encapsulate and immobilise its low and intermediate level waste streams within steel vessels of 500 L or larger [1,9]. Ground granulated blast furnace slag (GGBFS) and pulverised fuel ash (PFA) are SCMs that are employed both to enhance the performance of the wasteform, and to reduce the exotherm and the maximum temperature experienced by the mix, due to their slower rate of reaction in comparison to PC clinker [1,10]. Obtaining a consistent and standardised supply of these materials has become increasingly difficult throughout the past two decades, due to GGBFS being a by-product of iron production and PFA a waste generated from coal fired electricity generation; these are two industries that have undergone significant changes and that will continue to do so in the immediate future [10–12].

When combined with the ongoing development of alternative cements and the performance opportunities that these may afford, this has

* Corresponding author.
E-mail address: j.provis@sheffield.ac.uk (J.L. Provis).

https://doi.org/10.1016/j.conbuildmat.2023.131358
Received 9 January 2023; Received in revised form 3 April 2023; Accepted 6 April 2023
Available online 15 April 2023

Table 1
Rietveld analysis composition for Italcementi Alipre and Vicat Alpenat CK clinkers, showing significant phases.

Clinker compositions – Rietveld analysis				
Compound	Chemical formula	Cement nomenclature	Percentage identified in Alipre	Percentage identified in Alpenat
Ye'elimite	$Ca_4Al_6(SO_4)O_{12}$	$C_4A_3\overline{S}$	65.0	50.9
Belite (beta)	β-Ca_2SiO_4	C_2S	8.8	19.9
Belite (alpha)	α-Ca_2SiO_4	C_2S	8.9	8.1
Perovskite	$CaTiO_3$	CT	4.4	11.7
Merwinite	$Ca_3Mg(SiO_4)_2$	C_3MS_2	4.0	6.3
Anhydrite	$CaSO_4$	$C\overline{S}$	2.7	2.9
Fluorellestadite	3 $(2CaO{\cdot}SiO_2){\cdot}3CaSO_4{\cdot}CaF_2$	$C_{10}S_3\overline{S}_3\underline{F}_2$	1.7	–
Periclase	MgO	M	0.7	–
Bredigite	$Ca_7Mg(SiO_4)_4$	C_7MS_4	3.2	–
Quartz	SiO_2	S	0.5	0.2

led the UK nuclear industry to begin exploring alternative cementitious binder systems. CSA-belite cements are produced from a clinker that consists predominantly of ye'elimite, with a smaller proportion of belite. Ye'elimite is also commonly referred to as Klein's compound, and is the naturally occurring form of calcium sulfoaluminate, with the abbreviated cement chemical formula ($C_4A_3\overline{S}$) [1]. It is formed when an alumina-bearing material such as bauxite is heated with calcium sulfate and calcium carbonate. CSA is typically clinkered at between 1250 and 1350 °C, significantly lower than the PC clinkering temperature of 1450 °C [2,13]. This reduction is temperature is achievable in part due to the absence of alite (C_3S), responsible for the early strength development in PC. In CSA, this role is fulfilled by the hydration of ye'elimite [14]. The main product of hydration is expected to be ettringite (the archetype of the "AFt" – *tri* – phase family of hydrous calcium sulfoaluminates), with aluminium hydroxide (gibbsite or amorphous), formed through the consumption of both ye'elimite and an interground calcium sulfate source. In this study, the sulfate source is either anhydrite (Eq. (1)) or gypsum (Eq. (2))[1]. If a sufficient quantity of calcium sulfate is not available, then ye'elimite will hydrate to form calcium monosulfoaluminate, commonly referred to as monosulfate, and a representative of the "AFm" (*mono*) phase family (Eq. (3)).

$$C_4A_3\overline{S} + 2C\overline{S} + 38H \rightarrow C_3A \bullet 3C\overline{S} \bullet 32H + 2AH_3 \quad (1)$$

$$C_4A_3\overline{S} + 2C\overline{S}H_2 + 34H \rightarrow C_3A \bullet 3C\overline{S} \bullet 32H + 2AH_3 \quad (2)$$

$$C_4A_3\overline{S} + 18H \rightarrow C_3A \bullet C\overline{S} \bullet 12H + 2AH_3 \quad (3)$$

Ettringite has gathered interest for radioactive waste immobilisation, as it has been shown to act as a host for a number of radioactive and heavy metal waste ions [15]. This is achieved through hosting ions within the columnar and channel sections of the AFt crystal structure, as well as through substitution of the calcium (e.g. by Ba^{2+}), aluminium (e.g. by Cr^{3+}), hydroxide, and sulfate sites (e.g. by IO_3^- and AsO_4^{3-}) [15–18]. Ettringite crystals form in hexagonal prismatic columnar morphology, and have a water content of 30 – 32 mol H_2O per mole of Al_2O_3 ($C_6A\overline{S}_3H_{32}$) [15,19]. In PC, ettringite is formed early in the hydration reaction sequence, and provides much of the mechanism for the initial setting of the cement. The rate at which ettringite forms, and the greater quantity produced by CSA hydration, enables these cements to exhibit a much higher early strength when compared to PC [20,21]. The ettringite component is key to the overall stability of CSA. Studies of ettringite have shown a sensitivity to both the availability of water and temperature, which may cause dehydration and a reversible transition to meta-ettringite or decomposition into calcium monosulfate [17,19,22–25]. Jiménez *et al.* [17] show that the stability of naturally occurring ettringite outperforms that of synthetic ettringite, and so it is important that stability of ettringite can be established in a large scale series of commercially applicable cementitious formulations [17,24].

Belite, (C_2S), is responsible for the later-stage strength development of PC. Similarly, in CSA-belite cements, belite also hydrates relatively slowly. Hydration of belite forms either calcium silicate hydrate (C-S-H) (Eq. (4)), which has also been shown to be able to host a number of waste ions, or the silica-substituted AFm phase strätlingite (Eq. (5)) [15,26]. Belite hydration in the absence of aluminium hydroxide forms C-S-H and portlandite (calcium hydroxide), which could increase the pH of the pore solution (Eq. (4)) and the corrosive potential of some encapsulated metals such as aluminium, which is a common constituent of nuclear sector wastes and which corrodes at elevated pH. Belite has been shown to take in excess of three months to begin to react to a significant extent in a belitic CSA cement system, but appears to improve compressive strength once the slow process of hydration has begun [6].

$$C_2S + 2H \rightarrow \text{C-S-H} + CH \quad (4)$$

$$C_2S + AH_3 + 5H \rightarrow C_2ASH_8 \quad (5)$$

This paper reports upon the development of the hydrate assemblage of CSA-belite type cements, based on two commercial clinkers and different sources and levels of sulfate addition, at between 7 and 90 days and on the scale of a 3-litre mix. The impact of different concentrations of anhydrite or gypsum, different water to cement ratios, and different mixing shear regimes are all examined. The 40 mixes in this experimental series have been conducted in order to identify robust formulations of commercially available CSA-belite cements that can be utilised by the UK nuclear industry. A wide scope of successful mixes will demonstrate just how robust CSA can be, as well as allowing for future studies to be conducted upon a much larger scale, approaching the 500 L mixes conducted by the UK nuclear industry for waste encapsulation [9].

The key aims of this study are therefore: to establish the behaviour of the CSA-belite system within a larger mix formulation envelope than is commonly considered in academically-focused studies and up to 90 days of curing; to identify if the key ettringite phase has remained stable across this mix envelope; and thus to assess whether CSA is robust enough for consideration within the UK nuclear sector, while adding to the fundamental knowledge and experience of using CSA cements.

2. Experimental

2.1. Materials

Two commercial CSA-belite clinkers were selected; Alipre supplied by the Italcementi Group, and Alpenat CK supplied by Vicat Cement. The clinker composition was provided by the manufacturers, and a Rietveld analysis of a raw clinker sample was conducted to confirm this (Table 1). The Alipre clinker contains a relatively high ye'elimite content and low belite, while the Alpenat clinker is not quite so rich in ye'elimite and with a much higher belite content. Air permeability (Blaine) tests established that the powder finenesses of Alipre and Alpenat clinkers were 528 and 530 m^2/kg, respectively, with loss on ignition values of 0.87% and 0.50% respectively [27]. The calcium sulfate was used in the form of either anhydrite or gypsum, both supplied by Saint-Gobain Construction Products, and Table 2 shows the cement phase fractions recalculated to include the calcium sulfate. The reference files used to conduct Rietveld analysis of the XRD data are given in Table 3. The anhydrite and gypsum exhibited Blaine finenesses of 452 and 385 m^2/kg, respectively. No additional additives were used.

[1] Chemical reaction equations in this paper are presented using cement chemistry abbreviated notation, where C represents CaO, A is Al_2O_3, S is SiO_2, H is H_2O, and $\overline{S}$ is SO_3.

Table 2
Identified clinker compound percentages when theoretically adjusted for the calcium sulfate addition.

Compound	Alipre	Alpenat	15%		25%		35%	
Ye'elimite	65.0	50.9	55.3	43.3	48.8	38.2	42.3	33.1
Belite (beta)	8.8	19.9	7.5	16.9	6.6	14.9	5.7	12.9
Belite (alpha)	8.9	8.1	7.6	6.9	6.7	6.1	5.8	5.3
Perovskite	4.4	11.7	3.7	9.9	3.3	8.8	2.9	7.6
Merwinite	4.0	6.3	3.4	5.4	3.0	4.7	2.6	4.1
Anhydrite	2.7	2.9	2.3	2.5	2.0	2.2	1.8	1.9
Fluorellestadite	1.7	–	1.4	–	1.3	–	1.1	–
Periclase	0.7	–	0.6	–	0.5	–	0.5	–
Bredigite	3.2	–	2.7	–	2.4	–	2.1	–
Quartz	0.5	0.2	0.4	0.2	0.4	0.2	0.3	0.1

Table 3
Sources of the CIF files used from literature in order to conduct the Rietveld analysis.

Phase	Identification	Authors
Ettringite	155395-ICSD	F. Goetz-Neunhoeffer and J. Neubauer [28]
Gibbsite	6162-ICSD	H. Saalfeld and M. Wedde [29]
Monosulfate (kuzelite)	0014757-AMCSD	R. Allmann [30]
C-S-H (hillebrandite)	0001745-AMCSD	Y. Dai and J. Post [31]
Ye'elimite	80361-ICSD	N. Calos et al. [32]
Anhydrite	16382-ICSD	A. Kirfel and G. Will [33]
Gypsum	230283-ICSD	T. Fukami et al. [34]
Belite α (orthorhombic)	81097-ICSD	W. Mumme et al. [35]
Belite β (monoclinic)	81096-ICSD	W. Mumme et al. [35]
Portlandite	15471-ICSD	H. Petch [36]
Quartz	41414-ICSD	G. Will et al. [37]
Lime	52783-ICSD	D. Smith and H. Leider [38]
Hemihydrate	79528-ICSD	C. Bezou et al. [39]
Perovskite	62149-ICSD	S. Sasaki et al. [40]
Merwinite	431125-ICSD	X. Bao et al. [41]
Fluorellestadite	97203-ICSD	I. Pajares et al. [42]
Periclase	9863-ICSD	S. Sasaki et al. [43]
Bredigite	0000494-AMCSD	P. Moore and T. Araki [44]
Strätlingite	69413-ICSD	R. Rinaldi et al. [45]

2.2. Mix proportions and curing

In this study, results are generated from a total of 40 mixes, each of 3 L. The clinkers were blended with additional anhydrite or gypsum at levels of 15, 25, or 35 wt% of the total pre-blended solids in the mix design. The water to solids mass ratio (w/s), calculated on the basis of total solids (clinker + calcium sulfate), was set to either 0.5, 0.6 or 0.7 to enable the mixes to be produced with desirable flow and setting time characteristics, and mixed using either a low or high shear mixing method. Pre-blended solids were added to deionised water in a Hobart N50 mixer, operating at 62 rpm, over a period of 5 min, with mixing then continued for a further 5 min. At 10 min from the point of powder addition, high shear mixes were switched to a Silverson L5 mixer operating at 4500 rpm for 10 min. Low shear mixes remained at 62 rpm throughout the 20-minute mix duration. After this period, additional mixing was carried out at 62 rpm for up to a maximum of 150 min. Low and high shear mix methods were developed to represent the parameters and duration of a mix that is achievable and necessary using the full 500 L scale equipment and infrastructure currently employed in UK radioactive waste encapsulation, and to see if either shear method affects the phase assemblage within this time period.

Fluidity assessments were made every 30 min using a grout flow trough, whereupon mixes would be concluded and samples cast if a grout fluidity measurement of ≤500 mm was obtained. Samples used in this study were cast in 15 mL plastic centrifuge tubes, then cured at 20 ± 1 °C in a high humidity (>90% RH) walk in chamber, before being demoulded and undergoing solvent exchange to remove all free water content at the appropriate test date (7, 28, or 90 days) [46]. The use of sealed specimens is intended to replicate the autogenous environment within a wasteform in a sealed drum, and is a potential reason why no expansion was observed for the mixes in this study. The remainder of the 3-litre mix was used to produce studies for separate studies of rheological and mechanical properties, which are beyond the scope of this paper.

2.3. Ample preparation

A solvent exchange method using isopropanol was used to arrest hydration, as proposed by Scrivener et al. [46]. Free water was removed by submerging samples in isopropanol, which was routinely changed over a period of hours, with samples then being dried to constant weight in a desiccator [46]. For analysis by powder X-ray diffraction (XRD) and thermogravimetric analysis (TGA), samples were ground to a powder and sieved to <63 μm. Samples were kept under vacuum in a laboratory desiccator thereafter, isolated in sealed bags within the desiccator. All procedures were conducted and at a room temperature of approximately 20 °C.

2.4. Scanning electron microscopy (SEM) and energy dispersive X-ray spectroscopy (EDS)

Samples for SEM and EDS were sectioned into ~5 mm^3 slices before being cold mounted in epoxy resin. These samples were then ground and polished, using isopropanol as a lubricant, up to a 0.25 μm diamond grade. Samples were then carbon coated in a vacuum and given conductive silver paint tracks in order to prevent overcharging. SEM and EDS analysis were carried out by using a Hitachi TM3030 instrument, with EDS conducted using a Quantax 70 detector. Images were taken at magnifications of 250×, 500×, 1000× and 2500×, using an electron accelerating voltage of 15 kV and a working distance of 8 mm. EDS was conducted for all samples at 2500× magnification, and identified Al, Ca, Fe, Mg, Na, Si and S.

2.5. Thermogravimetric analysis (TGA)

TGA was conducted on <63 μm powdered samples using a Perkin Elmer TGA 4000. Testing involved 40 ± 2 mg samples in alumina crucibles, under an inert nitrogen atmosphere, at a heating rate of 10 °C/min from room temperature to 1000 °C. Analysis was conducted using the Pyris Manager software.

2.6. X-ray diffraction (XRD) and Rietveld analysis

XRD was conducted on <63 μm powdered samples, using a Panalytical X'pert3 instrument with Cu-Kα radiation. Sample holders were backloaded to reduce the degree of preferred crystal orientation. These samples were analysed over the 2θ range of 5 – 70°, at a step size of 0.026° and a time per step of 4 s. Quantification via Rietveld analysis

Table 4
Rietveld analysis results displaying the weight percentage (%) of each phase detected, for all 120 mixes that contain either Alipre clinker (Ali) and Alpenat CK clinker (Alp) clinkers. Inert phases detected, or those that could be classed as minor, were omitted. The full list of phases identified is given in Table 3.

Calcium Sulfate Type	Sulfate Content	w/s Ratio	Shear	Days	Ye'elimite		Belite		Anhydrite		Gypsum		Ettringite		Gibbsite		Mono-sulfate	
					Ali	Alp	Ali	Alp	Ali	Alp	Ali	Alp	Ali	Alp	Ali	Alp	Ali	Alp
	Low (15%)			7	19	9	16	23	7	6	1	1	30	22	14	17	6	9
Anhydrite		0.5	Low	28	15	12	13	18	8	8	1	1	36	25	13	16	7	8
				90	14	11	13	19	9	8	1	1	36	27	14	15	7	8
	Low (15%)			7	17	12	12	21	10	6	1	1	33	22	14	16	7	9
Anhydrite		0.5	High	28	15	11	13	22	13	7	1	1	37	27	9	14	5	8
				90	15	13	13	17	10	4	1	2	35	27	12	16	6	9
	Low (15%)			7	13	10	16	20	6	6	1	1	34	28	16	15	7	10
Anhydrite		0.7	Low	28	12	14	13	20	5	4	1	1	39	29	15	15	7	7
				90	13	15	13	16	5	4	1	1	37	27	16	16	7	8
	Low (15%)			7	13	11	16	20	5	5	1	1	34	28	16	16	9	9
Anhydrite		0.7	High	28	12	14	14	21	4	5	1	1	37	27	14	15	7	7
				90	11	14	13	21	4	3	1	1	37	27	15	16	8	8
	Med (25%)			7	12	10	12	19	12	9	1	1	39	29	12	13	6	8
Anhydrite		0.6	Low	28	12	10	13	19	9	8	1	1	43	31	11	13	6	8
				90	11	12	12	17	11	13	1	1	42	28	11	13	6	6
	Med (25%)			7	12	10	13	20	12	11	1	1	39	25	11	14	6	8
Anhydrite		0.6	High	28	12	10	14	21	12	7	1	1	37	28	11	13	6	8
				90	12	10	12	19	13	8	1	1	41	27	9	15	4	9
	High (35%)			7	9	7	12	14	22	24	1	1	30	25	11	12	7	6
Anhydrite		0.5	Low	28	9	7	11	14	22	25	1	1	33	26	11	11	7	6
				90	7	8	10	15	26	16	1	1	34	30	11	10	5	7
	High (35%)			7	9	11	11	16	24	20	1	1	28	25	12	10	7	6
Anhydrite		0.5	High	28	7	7	11	15	24	21	1	1	32	25	11	13	7	7
				90	8	8	10	16	21	16	1	1	35	33	15	9	5	6
	High (35%)			7	9	7	10	15	24	18	1	1	36	29	8	11	4	7
Anhydrite		0.7	Low	28	9	7	11	14	18	18	1	1	42	34	8	8	5	5
				90	8	7	8	14	19	17	1	1	46	34	7	9	4	7
	High (35%)			7	9	10	11	17	21	16	1	1	39	28	9	11	5	7
Anhydrite		0.7	High	28	10	7	9	14	21	18	0	1	43	32	6	11	3	6
				90	10	7	8	12	26	15	0	1	48	34	3	10	1	7
	Low (15%)			7	17	9	17	21	3	2	3	3	30	23	16	19	7	10
Gypsum		0.5	Low	28	18	11	13	23	3	3	3	2	32	23	15	17	7	10
				90	17	11	12	22	3	3	4	1	34	26	16	17	6	9
	Low (15%)			7	17	12	15	21	2	2	3	4	30	26	16	16	9	9
Gypsum		0.5	High	28	14	14	14	17	3	3	4	2	34	27	16	17	7	9
				90	16	14	12	21	3	5	3	2	35	28	16	16	7	7
	Low (15%)			7	11	11	17	23	3	3	1	1	36	25	17	17	7	10
Gypsum		0.7	Low	28	11	9	14	21	3	2	1	1	40	29	14	18	7	9
				90	11	12	12	20	3	3	1	2	41	28	15	16	8	9
	Low (15%)			7	11	11	14	24	3	3	2	1	39	24	15	18	8	9
Gypsum		0.7	High	28	10	11	13	21	3	3	2	1	41	32	16	14	7	9
				90	11	12	13	16	3	3	1	1	39	38	16	13	8	8
	Med (25%)			7	11	13	15	20	3	3	6	3	35	30	15	14	8	7
Gypsum		0.6	Low	28	10	10	15	20	3	3	6	3	35	31	15	14	8	9
				90	10	9	13	20	3	3	4	3	41	36	15	13	7	7
	Med (25%)			7	13	10	14	19	3	3	6	4	39	31	13	14	6	8
Gypsum		0.6	High	28	13	10	15	20	3	3	4	2	40	32	12	14	6	8
				90	13	13	13	19	3	3	6	2	42	30	11	15	5	8
	High (35%)			7	11	9	11	19	3	2	17	10	36	23	11	15	6	10
Gypsum		0.5	Low	28	10	10	10	18	2	2	17	10	39	32	10	11	6	5
				90	10	10	9	14	2	3	15	7	43	32	10	14	4	9
	High (35%)			7	11	10	12	20	3	3	12	10	38	23	12	16	7	7
Gypsum		0.5	High	28	9	8	10	18	2	2	15	9	42	27	10	17	6	8
				90	11	7	10	16	3	2	13	9	44	29	10	16	5	8
	High (35%)			7	9	11	15	18	3	3	7	7	37	30	13	14	8	8
Gypsum		0.7	Low	28	8	12	13	16	3	3	7	9	41	32	14	12	6	6
				90	9	10	11	16	2	3	8	4	42	42	15	10	7	5
	High (35%)			7	8	10	15	16	3	2	9	8	38	33	12	11	8	8
Gypsum		0.7	High	28	8	13	13	17	3	3	7	5	42	33	14	13	7	7
				90	8	12	12	16	3	3	5	3	43	36	14	12	7	7

was conducted in the TOPAS software, for both unreacted clinkers and hydrated products, using the fundamental parameter approach for all phases and without the use of an internal standard. Ettringite values for comparable mixes, differing only in the shear history of the mix, were found to vary by an average of 2%, indicating good stability and reproducibility of the refinement methodology. An average R_{wp} value of 1.83 was generated from all refinements, indicative of a successful final structure model and refinement [47].

The calculation of error within the values generated by Rietveld analysis is difficult, especially in systems with a large number of phases, and may result in an error ranging from one to several percent or more [48]. A margin of error is best theorised using Table 2, where the percentage adjusted for the calcium sulfate addition is very occasional a couple of percent under what was identified in the hydrated sample. Quantification of accuracy must take into account instances of preferred crystal orientation, X-ray micro absorption, the amorphous phase content, the quality of the reference patterns, and any other potential factors [48,49]. Whilst these factors were mitigated where possible, the focus of

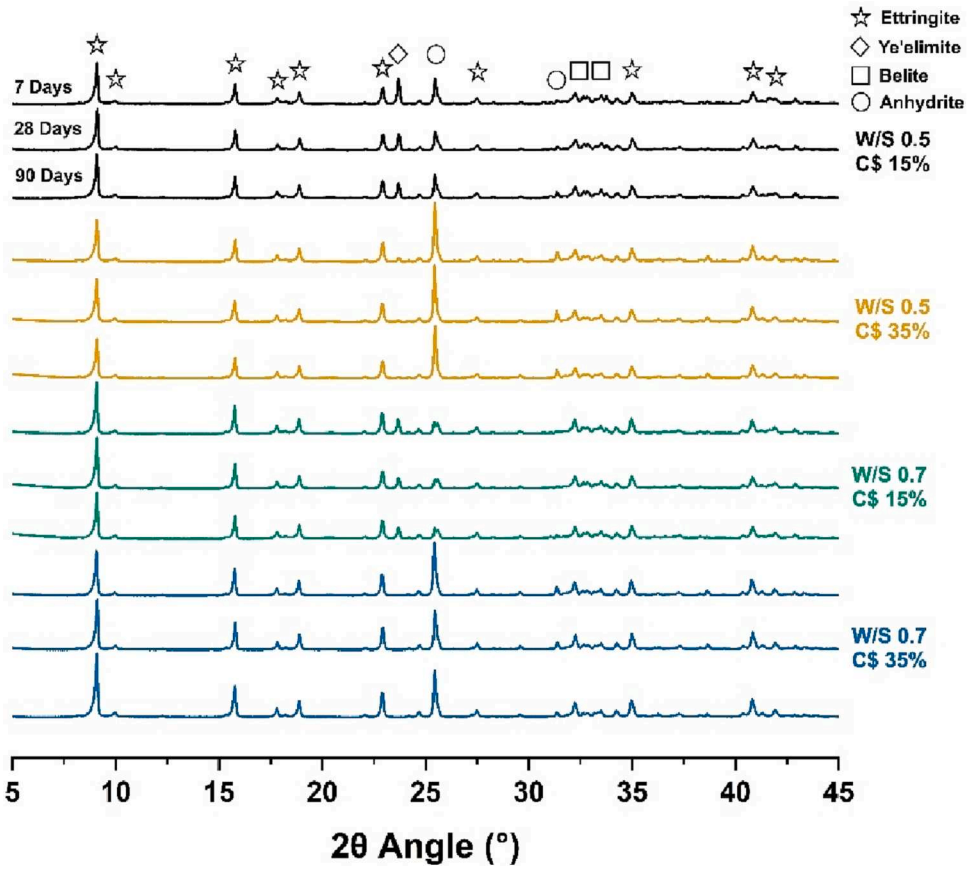

Fig. 1. XRD pattern for Alipre clinker, with anhydrite at either 15% or 35% and a w/s ratio of 0.5 or 0.7. Increased ye'elimite hydration can be observed by the decrease of the main peak at 23.7° 2θ with increasing calcium sulfate and water content. Background levels have been reduced, most notably preceding 8° 2θ, in order to generate this figure.

this paper will be a comparison between the extensive range of samples, produced in a controlled manner, covering several different key variables.

2.7. Thermodynamic modelling

Gibbs Energy Minimization Software (GEMS) was used in the form of CemGEMS, a browser-based application based upon the GEMS3K code, that allows the user to load and modify cement recipe templates and conduct computations using the Cemdata18 and PSI/Nagra databases [50]. The template available for CSA-belite cement is based upon the work of Jeong et al. [48], which was modified in order to reproduce the compositions of the Alipre and Alpenat clinkers, accompanied by the addition of appropriate calcium sulfate and water to match the experimental mixes. Component enthalpy values the their degree of hydration were retained as given in Jeong et al. [48]. Simulations were run to account for every change in mix parameters, except shear rate, at a pressure of 100 kPa and temperature of 20 °C. The duration was allowed to exceed 10,000 years, representative of the extremely long timescales that radioactive waste repositories will function [51]. Cement hydration as a function of time was plotted using the 5 parameter logistic (5PL) function, and was based around 100 g of clinker with the additional calcium sulfate then added [50]. The extent of reaction for each mix was calculated using the percentage of remaining ye'elimite identified by Rietveld analysis at 90 days, with an extent of reaction between 63% and 76% exhibiting the same quantity of ye'elimite remaining at 90 days, allowing for a model more representative of its experimental equivalent.

3. Results and discussion

3.1. Degree of hydration

3.1.1. Ye'elimite

Ye'elimite is the hydraulic phase primarily responsible for the production of ettringite when hydrated in the presence of sufficient calcium sulfate (Eqs. (1), (2)), and it is relatively rapidly consumed in the hydration of CSA-belite cements. The remaining weight percentage ye'elimite content, as identified by the Rietveld analysis of the solid product and compared against the quantity of ye'elimite present within each mix, at 90 days was between 7% and a maximum of 17% (Table 4). Quantifying the degree of reaction in Alipre clinker whilst accounting for the calcium sulfate addition, it is calculated that between 73% and 83% of the ye'elimite present has reacted with anhydrite during the first 90 days, or between 69% and 81% when the calcium sulfate source is gypsum. Correspondingly for the Alpenat clinker, between 65% and 79% of ye'elimite has reacted with anhydrite, and between 68% and 79% has reacted with gypsum. Gypsum dissolves faster than anhydrite, and has reportedly increased the rate ye'elimite dissolution and hydration within the first few hours [52,53]. At 7 days, the earliest point of measurement within this study, there is no clear indication that there is greater ye'elimite hydration in the presence of gypsum at this time period or beyond.

Within all mixes conducted, the majority of ye'elimite has been consumed through hydration. The proportion of ye'elimite consumption between Alipre and Alpenat clinkers is very similar, with Alipre only showing a small increase in the degree of ye'elimite consumption over Alpenat in most comparable mixes. The degree of ye'elimite hydration is linked strongly to the clinker being blended with an increasing quantity

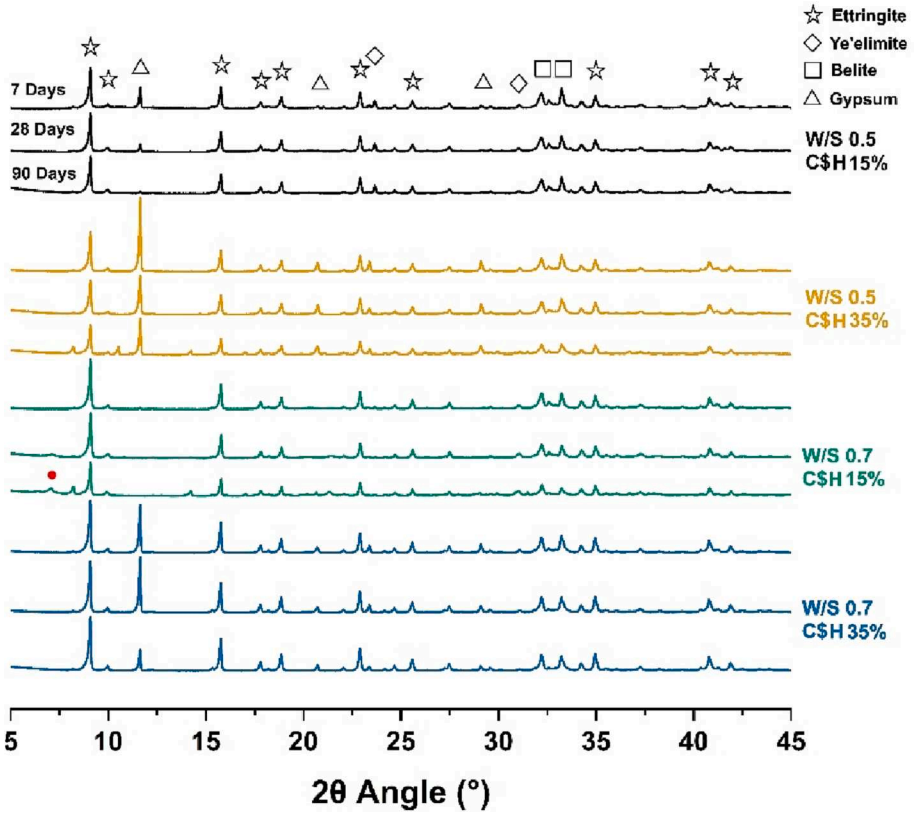

Fig. 2. XRD pattern for Alpenat clinker, with gypsum at either 15% or 35% and a w/s ratio of 0.5 or 0.7. The signature for strätlingite is visible at 7.2° 2θ, (red dot) in the low gypsum and high water mix at 28 days and beyond. Background levels have been reduced, most notably below 8° 2θ, in order to generate this figure. (For interpretation of the references to colour in this figure legend, the reader is referred to the web version of this article.)

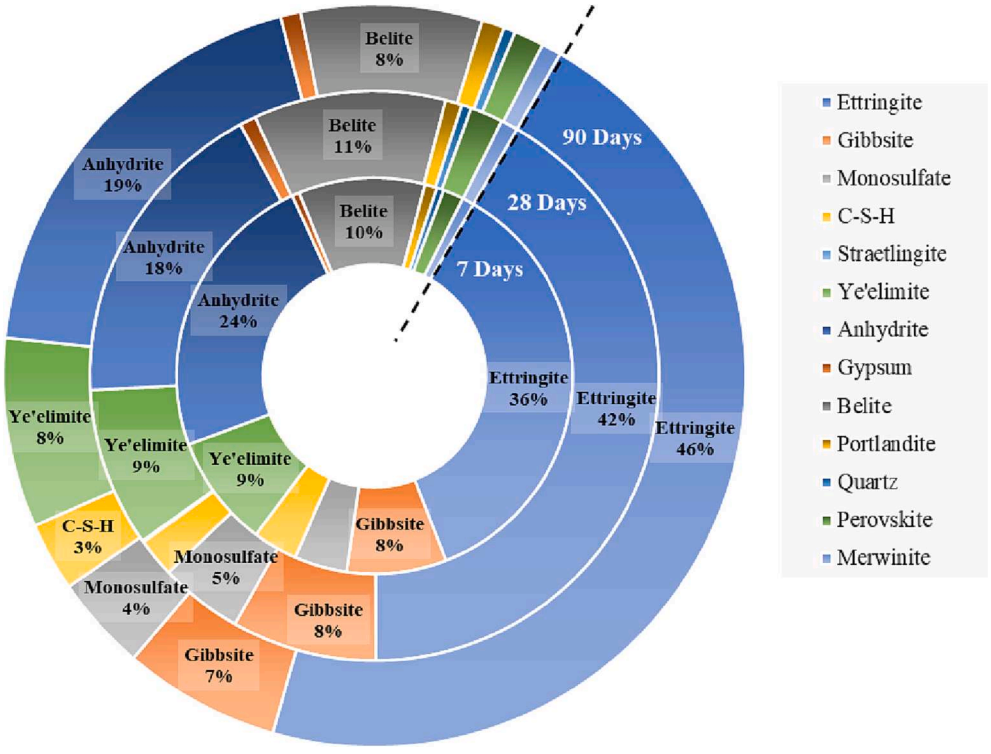

Fig. 3. This concentric Rietveld analysis plot, for an Alipre mix containing 35% anhydrite and a w/s ratio of 0.7, displays the weight percentage (%) of main phases detected over the 90-day period. Most notably, the increased production of ettringite between 7 and 28 days, as opposed to between 28 and 90 days, is clearly shown in this mix.

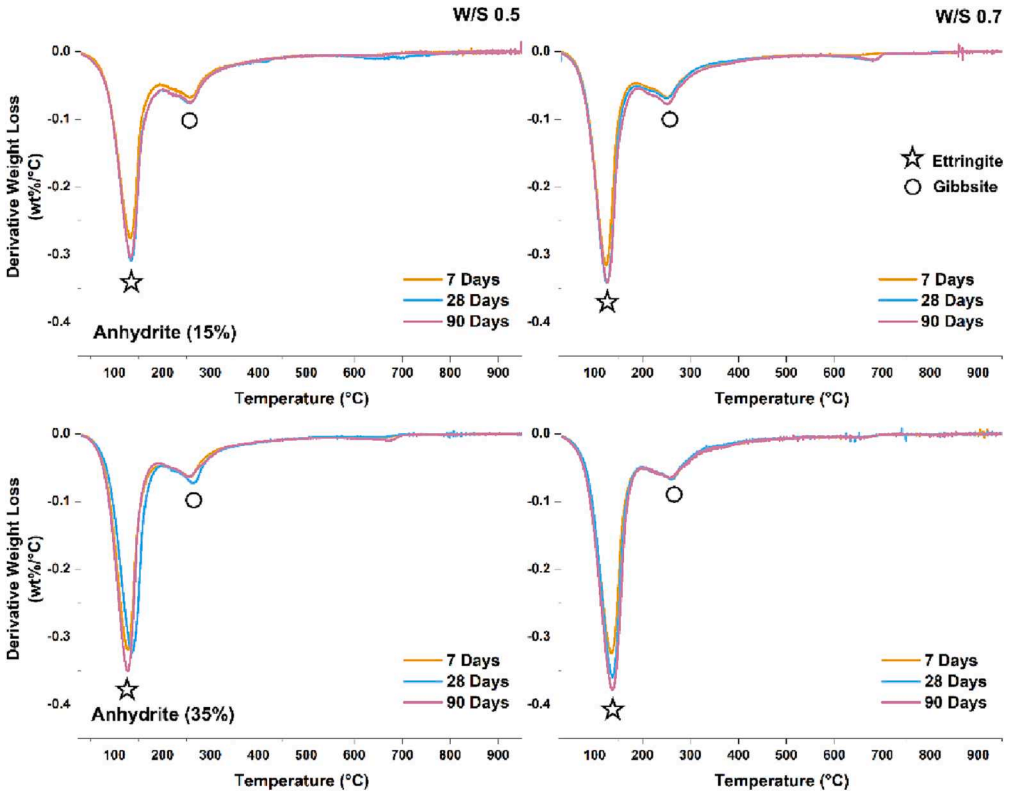

Fig. 4. TGA for Alipre clinker, with anhydrite at either 15% or 35% and a w/s ratio of 0.5 or 0.7. An increase in ettringite content is evident with an increase in anhydrite, as well as water.

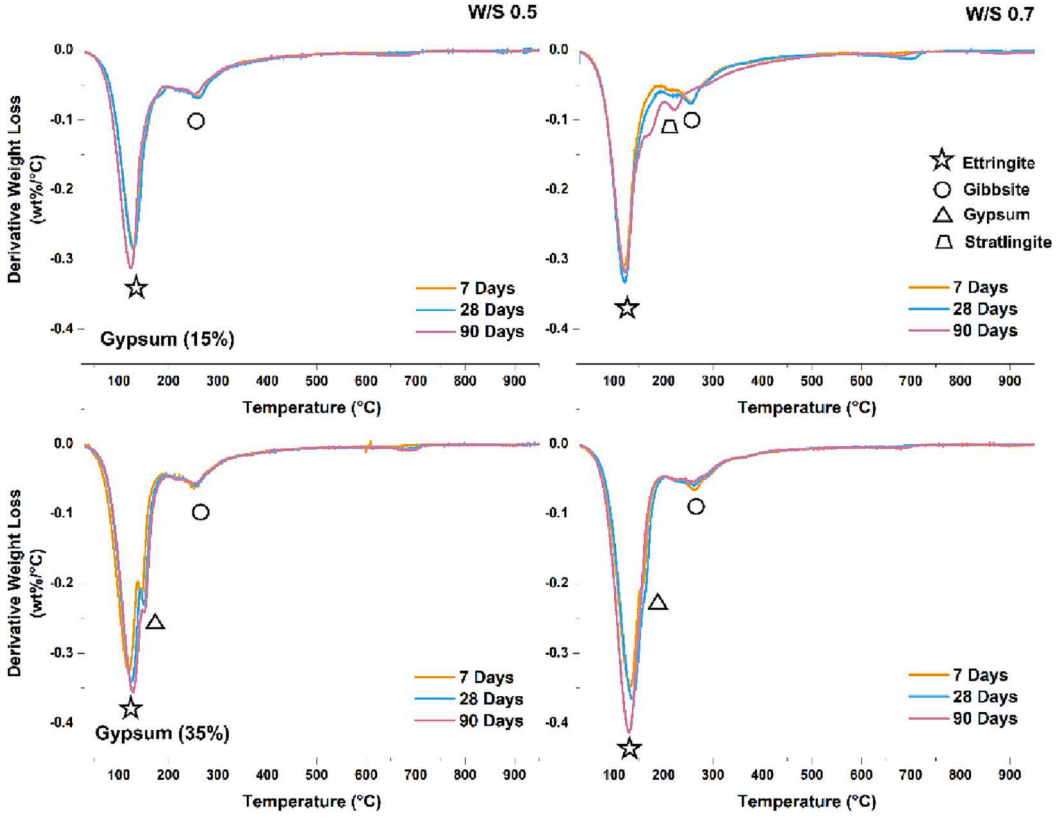

Fig. 5. TGA for Alpenat clinker, with gypsum at either 15% or 35% and a w/s ratio of 0.5 or 0.7. The signature for strätlingite is visible at approximately 220 °C in the low gypsum and high water mix at 28 days and beyond.

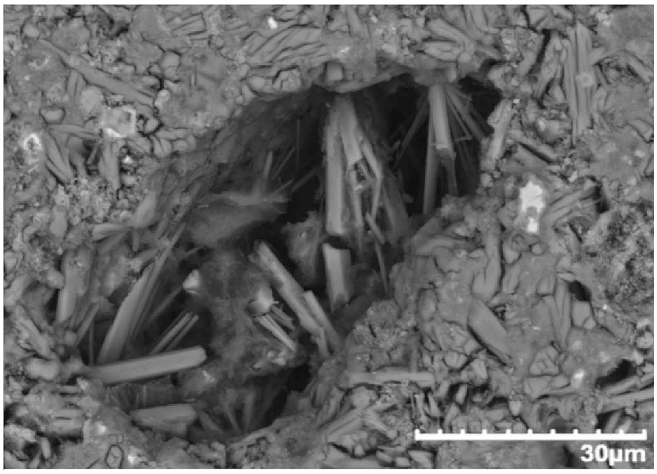

Fig. 6. An ettringite 'nest', where the lath shaped crystals have grown into a pore; a clear indication of ettringite growth after the initial setting of the Alpenat mix with low gypsum (15%) and a w/s ratio of 0.7. This sample was taken at 90 days.

of calcium sulfate. This is clearly shown in Figs. 1 and 2, with a sharp decrease in the main ye'elimite peak at 23.7° 2θ with increasing calcium sulfate content.

The availability of sulfate is reported to accelerate the hydration of ye'elimite within the first 24 h, as well as densifying the cement matrix with the rapid generation of hydration products [52–54]. Berger et al. [54] report that this densification of the matrix with fine ettringite crystals, which inhibits the passage of water to clinker particles, results in only minor hydration between 7 days and 1 year in systems with a w/s of 0.55. Ye'elimite hydration beyond 7 days is observed to be slight (Figs. 1 and 2), however in these systems there is an indication of consistent ettringite generation after 7 days and up until 90 days at a decreasing rate (Fig. 3). The slower reacting anhydrite could result in higher levels of hydration before densification takes place, however within this study there is little to distinguish between anhydrite and gypsum hydration over all mixing variables [52]. To a lesser extent than the calcium sulfate, the quantity of water available is also a contributing factor to the degree of ye'elimite hydration in most mixes, as most clearly shown in Fig. 1, between the w/s ratios of 0.5 and 0.7. There is no indication that the shear method used has had any effect upon the consumption of ye'elimite within the reported timeframe (Table 4).

3.1.2. Belite

The belite content within hydrated samples produced with both clinkers remains nearly constant, with only a small decrease over the 90-day period in all hydrated samples. Belite levels detected by Rietveld analysis in solid Alipre products are close to the initial belite content found in the clinker. Alpenat products have shown some consumption of belite, however the average quantity consumed is only 17% of the total amount within the mix at 90 days (Table 4).

The majority of the belite present in Alpenat is monoclinic (β-C_2S), with a minority of faster hydrating orthorhombic α-C_2S, and each being present in almost equal amounts in Alipre clinker (Table 1) [55]. The predominance of β-C_2S could be contributing to its low reactivity within the 90-day hydration period [6]. Jeong et al. [48] has also proposed that the rapid formation of ettringite could densify the matrix of the cement, whilst chemically binding (and thus consuming) water and limiting the diffusion of ions, which would explain the very low degree of belite hydration observed in the higher-ye'elimite Alipre system [56]. No relationship is evident between the type of calcium sulfate, the quantity of the calcium sulfate addition, or the water content of these mixes and the degree of belite hydration from the Rietveld analysis; however, in

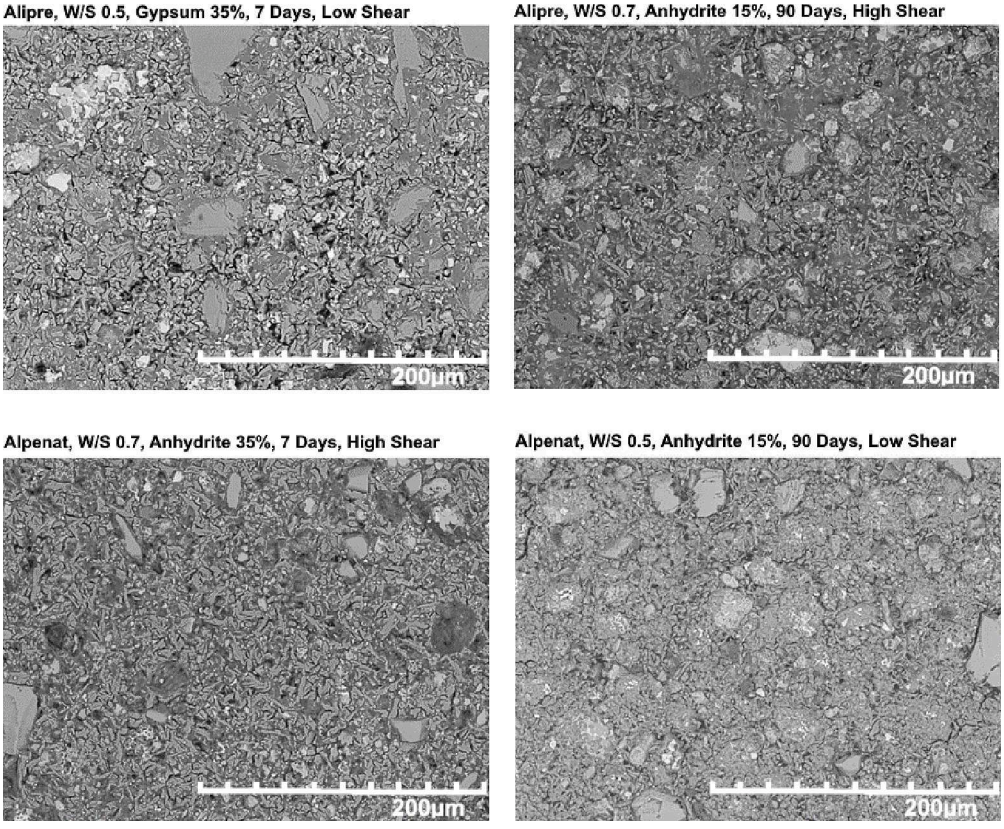

Fig. 7. SEM images showing very similar structures of ettringite lath crystals within an aluminium hydroxide matrix, between differing clinkers, types of calcium sulfate, and w/s ratios. Un-hydrated calcium sulfate and clinker particles can also be observed.

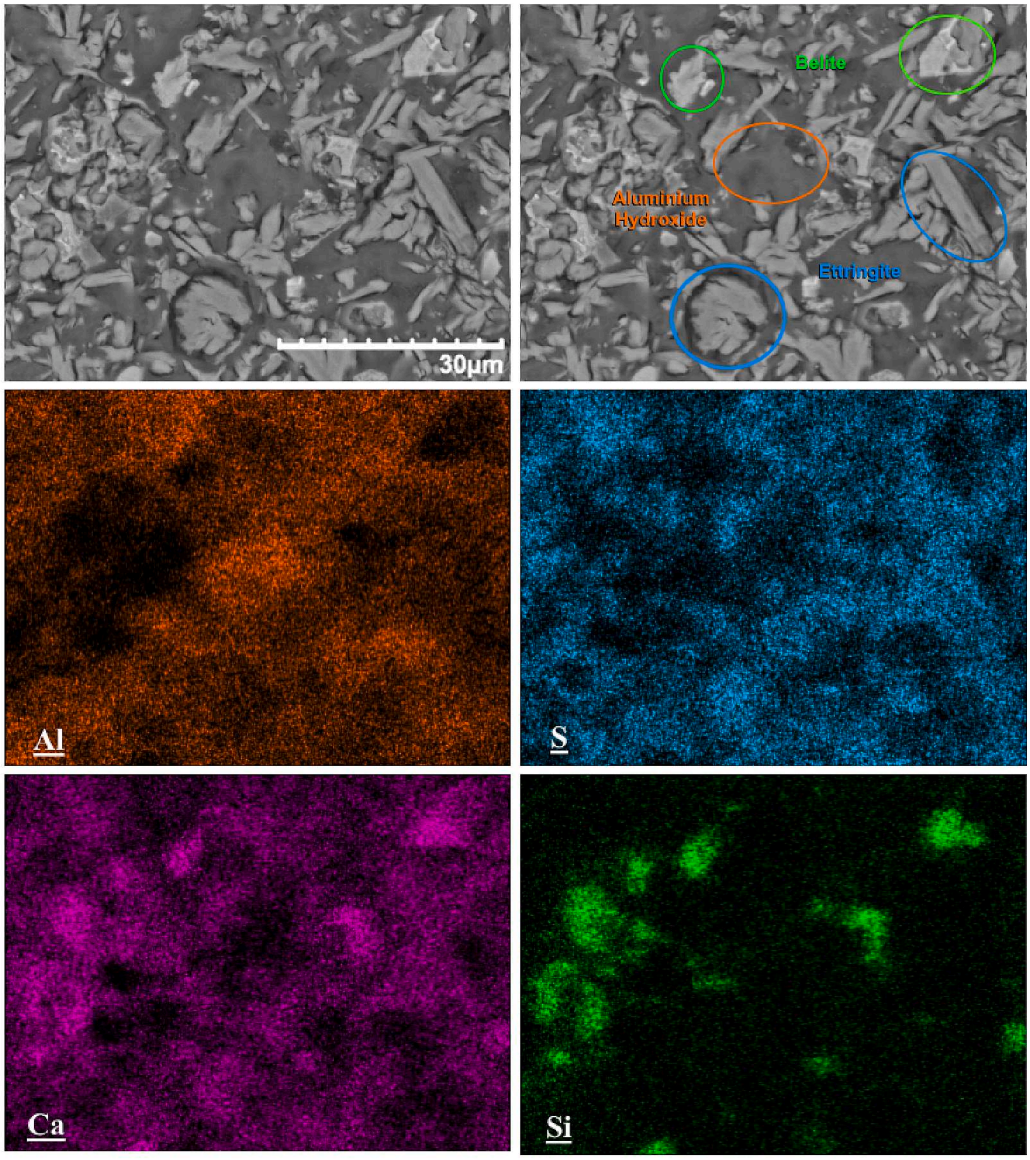

Fig. 8. SEM-EDS mapping of Alipre with high gypsum (35%) and a w/s ratio of 0.7. Ettringite, belite and aluminium hydroxide can clearly be identified their characteristic elemental signatures.

Alpenat there is an indication of strätlingite in XRD and TGA within 15% gypsum and 0.7 w/s ratio mixes (Figs. 2 and 5). This could be due to the greater overall availability of water for belite hydration, given that levels of ettringite production are lower at these formulations.

3.2. Ettringite formation

The production of ettringite is dependent upon the availability of ye'elimite, calcium sulfate and water. The absence or depletion of calcium sulfate will result in the production of monosulfate (in crystalline or disordered forms), and this reaction also has approximately half the water requirement of ettringite formation (Eq. (3)). The ettringite content of the hydrate assemblages resulting from both Alipre and Alpenat clinkers increases significantly with the addition of more calcium sulfate, consistent with expectations based on the reaction stoichiometry with respect to calcium sulfate. An increase in water availability, with a higher water to solids ratio, also increases the quantity of ettringite found. This is consistent with findings that similar CSA-belite systems have self-desiccated at a w/s ratio of approximately 0.5, with additional water allowing for additional production of ettringite [48,52]. In this experimental procedure however, there was no indication that self-desiccation occurred within any sample.

For both clinkers, there is also no real indication that anhydrite or gypsum produces consistently more ettringite than the other (Table 4). There is the potential for anhydrite to increase the quantity of ettringite present against the faster dissolving and thus faster reacting gypsum, due to gypsum quickly densifying the cement matrix with ettringite and hindering later hydration, but this has not been observed [54]. The quantity of ettringite formed by each clinker, when accounting for the quantity of ye'elimite present in each, is also similar. On average across all mixes, Alpenat mixes contained 24% less ye'elimite than Alipre mixes, and as a result there is a 22% less yield of ettringite after 90 days.

The majority of ettringite formation in all mixes occurs at 7 days or before, with a maximum increase in the content of ettringite of only 12% between 7 and 90 days (Alpenat, w/s 0.7, 35% gypsum). More ettringite formation occurs earlier (7 days or before) in mixes with higher water/

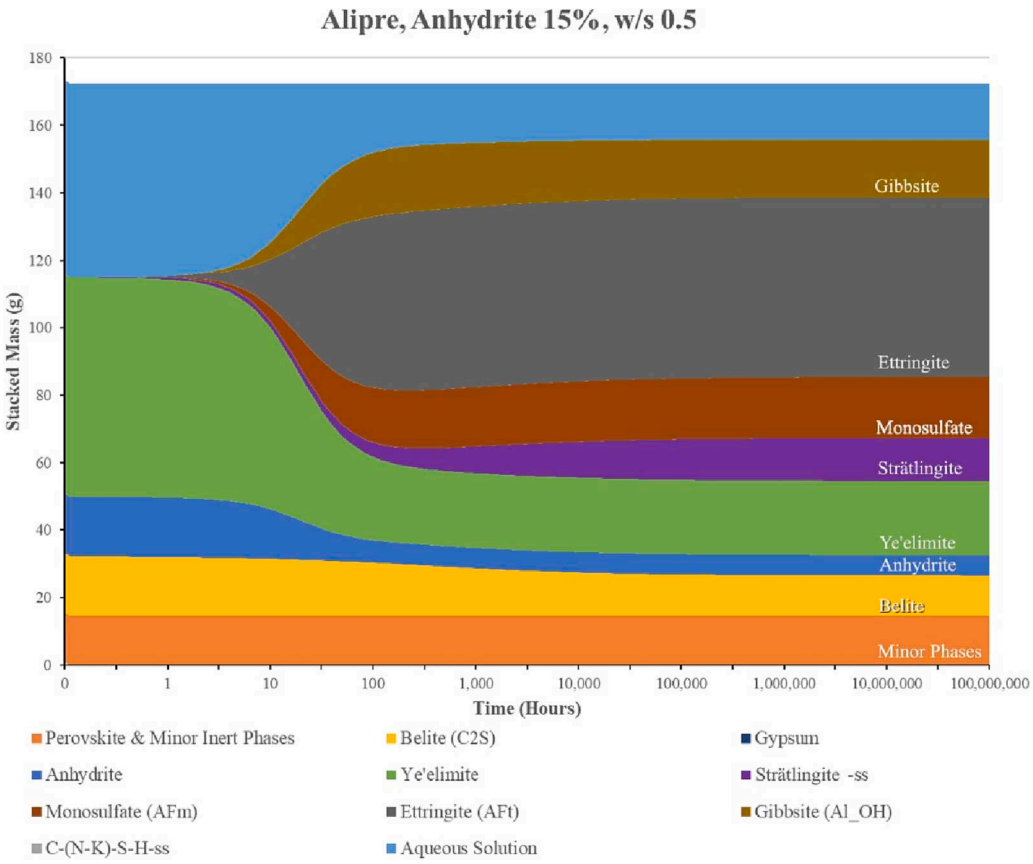

Fig. 9. CemGEMS simulation for Alipre clinker at an anhydrite addition of 15% and a w/s ratio of 0.5. The level of hydration, so as to be comparative to experimental results, was set to 66%. Anhydrite levels are predicted to become depleted, leading to the generation of monosulfoaluminate.

cement ratio. This could be due to the higher water availability being able to overcome the densification of the system which may hinder later hydration [52,54]. The later formation of ettringite, occurring after the initial setting, is demonstrated in Fig. 6. This SEM image shows numerous ettringite crystals that have formed after the initial setting. The porosity shown has formed during the initial setting, with the characteristically lath shaped ettringite crystals growing and spanning the width of this pore after it has formed.

3.3. Phase assemblage

SEM and EDS images, as exemplified in Figs. 6, 7, and 8, show large networks of ettringite crystals within a matrix of aluminium hydroxide. Ettringite is clearly identifiable by its lath-shaped crystals, and by the high concentration of Ca and S with an absence of Al or Si. The aluminium hydroxide matrix is identifiable by the strong concentration of Al distinct from other phases within the system. Unreacted belite and other minor clinker constituents can also be observed. Ca and Si EDS maps show high concentrations confined to very specific areas, with a minor distribution of silicon elsewhere in the sample, suggesting that the silicon is largely limited to the unreacted belite particles identified. For both clinkers, a significant majority of the Si is within the belite phases (Table 1).

Furthermore, there is evidence to suggest that ettringite stability during the hydration period for all samples has been high under the curing and storage conditions used. Rietveld analysis shows an increase in ettringite content over time, with no strong indication of ettringite decreasing; ettringite having shown to be forming within the pore structure after the initial set (Fig. 6).

The TGA results also give evidence to support that the levels of ettringite have not decreased over time [57]. The derivative weight loss that occurs at approximately 120–130 °C for ettringite shows that the level of ettringite increases with increased water and sulfate content. As also shown in the Rietveld analysis above, there is little to separate between the type of calcium sulfate or clinker used. In all instances, there is a small increase in the peak rate of weight loss at 90 days when compared to 7 days, indicating an increase in the quantity of ettringite over time (Figs. 4 and 5) as discussed above.

Levels of monosulfate remain at a near constant level throughout the hydration periods of each mix as identified in the Rietveld analysis (Table 4) [22,58]. A significant increase in monosulfate formation could be taken as an indication of the decomposition of ettringite [58]. TGA does not display any significant indication of monosulfate at 150 °C, which would be displayed as a shoulder on the peak attributed to ettringite (Figs. 4 and 5). The decomposition of ettringite to monosulfate would also result in the precipitation of calcium sulfate [22,58]. The levels of anhydrite and gypsum identified in the Rietveld analysis remain largely constant over time. Rietveld/XRD and TGA each show large quantities of calcium sulfate remaining after 90 days in the higher (35%) calcium sulfate samples, with some residual quantities detected even at the lowest (15%) sulfate addition. Remaining quantities of calcium sulfate shown in the Rietveld analysis more than double in the 35% sulfate mixes, when compared to the 25% sulfate mixes (Table 4). Similar levels of residual calcium sulfate were also observed by Berger et al. [54], where gypsum levels remaining at 7 days were approximately 4% for a 20% addition to the clinker, and 15% for a 35% addition at a w/s ratio of 0.55.

Levels of aluminium hydroxide detected by Rietveld analysis do not increase in line with ettringite, but rather remain at a consistent level. This could in part be due to the sometimes-amorphous structure of aluminium hydroxide being difficult to detect using XRD, and any change in quantity being difficult to differentiate by its small TGA

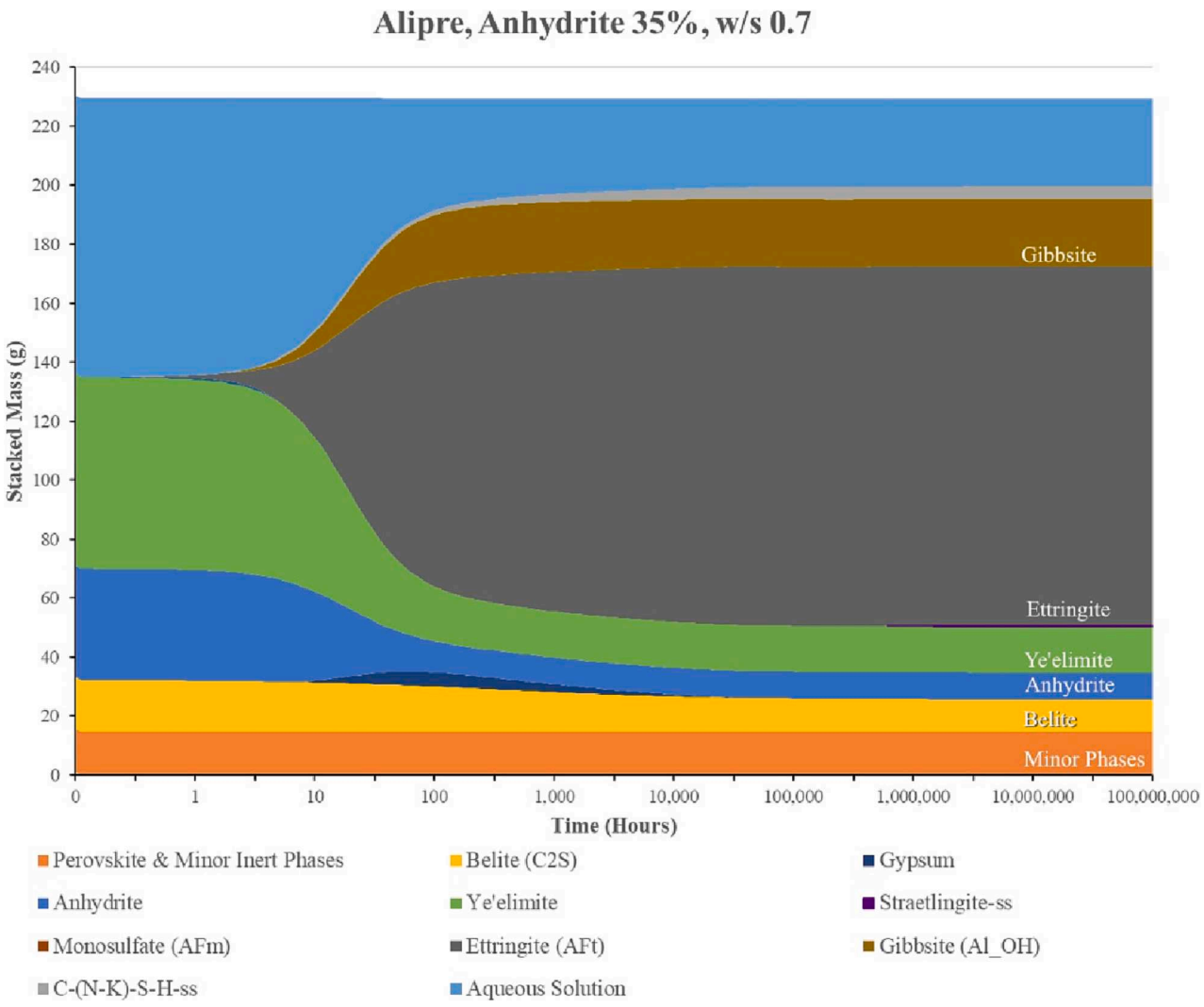

Fig. 10. CemGEMS simulation for Alipre clinker at an anhydrite addition of 35% and a w/s ratio of 0.7. The level of hydration, so as to be comparative to experimental results, was set to 76%. The potential for late stage belite hydration is shown as a small quantity of strätlingite formation.

signature. It is also consumed in the hydration of belite to form strätlingite (Eq. (5)).

3.4. Belite hydration products

The high quantity of remaining belite observed within both clinkers suggests that a large proportion has not yet hydrated. This is also evident given the lack of belite hydration products detected in the majority of samples. The C-S-H content identified in the Rietveld analysis was consistently low at an average of 3%, and negligible strätlingite was detected; however, the amorphous structure of C-S-H can make identification using XRD difficult, whilst the main strätlingite peak occurs at 7.2° 2θ in a range susceptible to high background noise. The distribution of calcium and silicon in EDS shows high concentrations confined to very specific areas, with a minor distribution of silicon elsewhere in the sample (Fig. 8). This would suggest that the silicon concentration is limited to the unreacted belite particles identified.

The hydration of belite without the presence of aluminium hydroxide generates C-S-H along with calcium hydroxide, which could be responsible for a later-age increase in pH in some CSA-belite cements (Eq. (4)). The quantities of C-S-H and portlandite identified by Rietveld here are consistently low, with an average across all mixes of 3% and 1% and 90 days, respectively. The consistency of this generation could potentially be due to the similar quantities of faster reacting α-C_2S being present across all mixes. C-S-H is also not clearly identifiable in the TGA, and whilst it would dehydrate at a similar temperature to the main ettringite peak and AFm of approximately 150 °C, there is no significant shoulder to this peak that would suggest a strong secondary phase within this TGA curve. Gypsum also strongly occupies this region (Fig. 5). The significance of a presence of calcium hydroxide brought about by the generation of C-S-H needs to be fully understood if these cements are to be used in encapsulation of some classes of wastes which are not compatible with highly alkaline conditions. Jeong et al. [48] however, do suggest that strätlingite is the primary long term hydration product of belite in the presence of aluminium hydroxide (Eq. (5)), the example clinker in that study having ye'elimite and belite contents similar to Alipre here (Table 1) [48,59].

Similar to C-S-H, the Rietveld, as well as the XRD and TGA cannot identify any significant strätlingite, with two noticeable exceptions. Alpenat mixes which feature the higher belite content, when combined with the highest water content (0.7 w/s) and the lowest gypsum content only (15%), exhibit a small but characteristic main strätlingite peak in the XRD at 7.2° 2θ (Fig. 2) and the indicative derivative weight loss in the TGA after 28 days (Fig. 5) [6,59]. Smaller XRD indications of strätlingite are also noticeable in some low-calcium sulfate Alpenat mixes at 90 days. This supports the observations of Jeong et al. wherein the production of ettringite hindered the hydration of belite [48]. There is a potential, therefore, that Rietveld analysis has been unable to

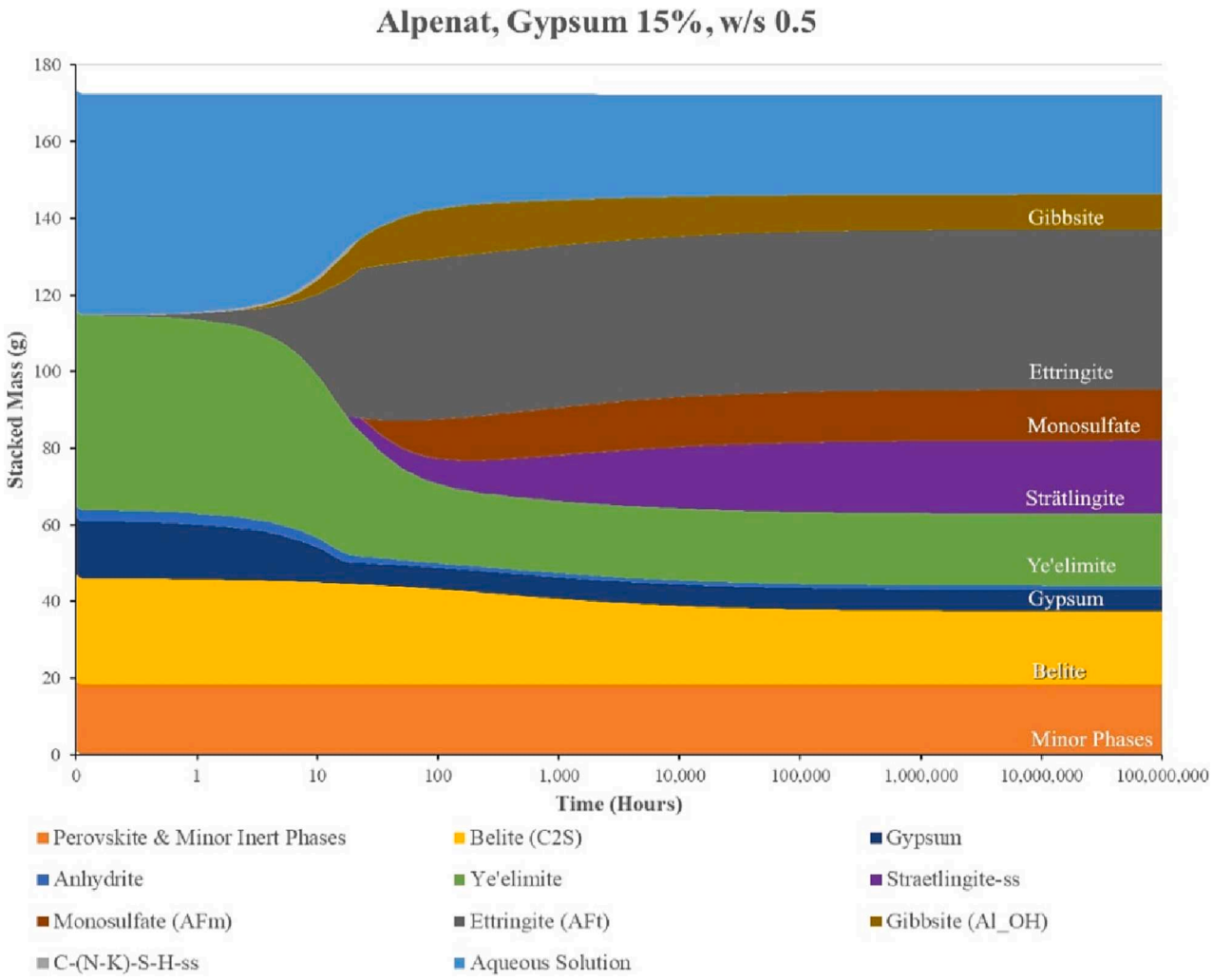

Fig. 11. CemGEMS simulation for Alpenat clinker at a gypsum addition of 15% and a w/s ratio of 0.5. The level of hydration, so as to be comparative to experimental results, was set to 63%. The increased quantity of belite when compared to Alipre clinker, has allowed for Alpenat to form more strätlingite, though a significant proportion remains unreacted. >1% C-S-H has been simulated up until 20 h, where it is succeeded by the appearance of monosulfate and the increasing quantity of strätlingite.

identify the formation of strätlingite in these cases due to high background signal below 8° 2θ.

3.5. Thermodynamic modelling

Thermodynamic modelling conducted using CemGEMS [50] predicts a phase assemblage largely similar to that identified by the Rietveld analysis and complemented by the other analytical methods, as well as past studies that applied thermodynamic modelling to CSA-belite cements [48,60]. Ettringite and aluminium hydroxide (in the form of gibbsite) are majority phases, as has been determined practically. Two phases differ significantly between the simulations and the experimental mixes: the quantities of monosulfate, and that of strätlingite, most notably in 15% calcium sulfate mixes (Figs. 9 and 11). The quantities of these phases within these simulations are much larger than that observed within the Rietveld analysis, with negligible strätlingite detected in all experimental mixes, although other indications of strätlingite having been identified.

Monosulfate, formed when ye'elimite reacts in the absence of sufficient calcium sulfate (Eq. (3)), decreases sharply in simulations when levels of calcium sulfate addition are raised above 15%, to the extent that it is entirely absent in 35% simulated mixes (Figs. 10 and 12). Whilst this deviates from what is seen in the Rietveld analysis, monosulfate levels do remain stable, with no more than a 1% increase within the mix between 7 days and the full duration of the simulation. There is, therefore, no significant amount of monosulfate generation, or consumption to form further ettringite within both simulated and experimental mixes. The increased levels of strätlingite are a function of the increased belite hydration, however residual belite levels are very similar to those identified in the experimental mixes. Strätlingite levels also significantly decrease with increasing ettringite formation, which corresponds to the findings of Jeong et al. [48], strätlingite preferring lower calcium sulfate mixes [61]. Also of note, a small quantity of C-S-H is formed at high calcium sulfate regardless of the water content, potentially driven by this preference, with the increased generation of C-S-H having not been identified experimentally (Figs. 10 and 12).

Simulations have shown the levels of ettringite greater than that identified by Rietveld, however they do remain at a near constant level past 90 days with a smaller corresponding quantity of aluminium hydroxide. Ettringite levels only increase, with no indication of any decomposition. Levels of residual calcium sulfate and ye'elimite also appear to remain near constant after 90 days. The quantity of ettringite also appears to increase strongly with increasing levels of calcium sulfate within that 90-day timeframe, as has been observed in the Rietveld analysis. There were no cases of self-desiccation shown within any of the simulations, with a small increase in water consumption for anhydrite

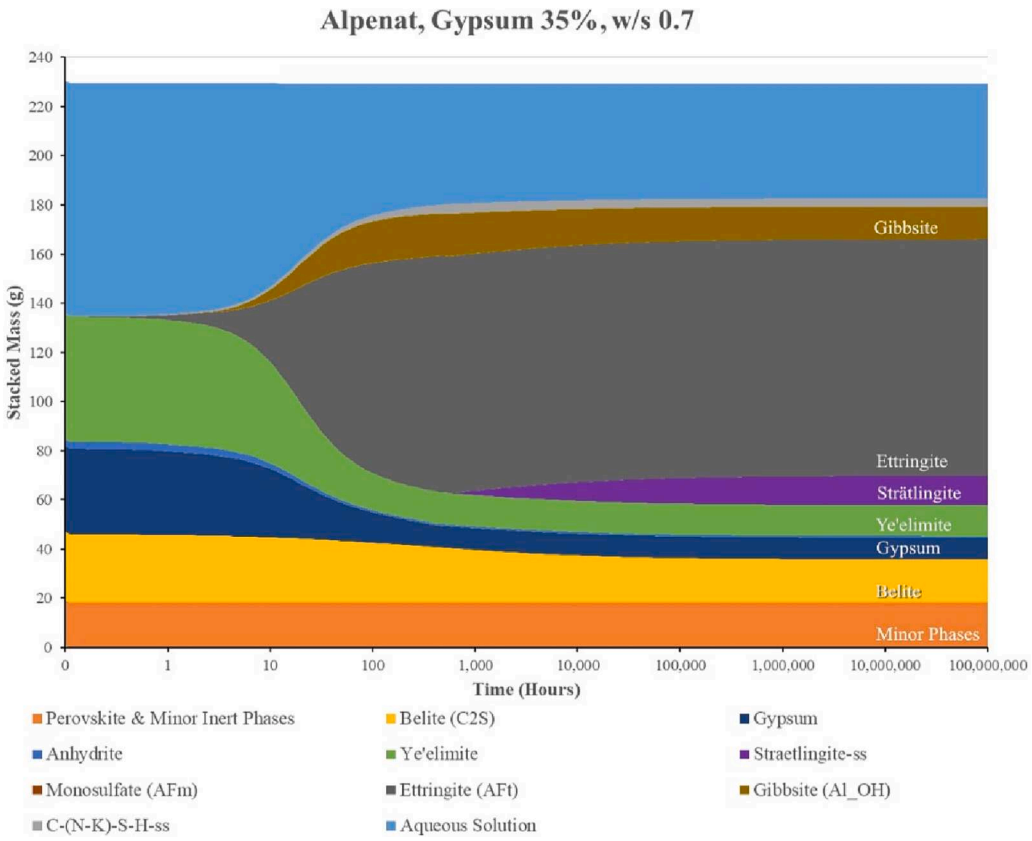

Fig. 12. CemGEMS simulation for Alpenat clinker at a gypsum addition of 35% and a w/s ratio of 0.7. The level of hydration, so as to be comparative to experimental results, was set to 75%. Increase ettringite formation has likely hindered belite hydration, however; some belite hydration has occurred without the presence of gibbsite, forming C-S-H (Eq.4).

mixes as also identified in the findings of Cau-dit-Coumes et al. [52].

As mentioned above, high levels of unreacted belite remain beyond the 90-day period. The belite phase, however, is the only phase to show significant signs of further reactivity beyond 90 days, albeit on a small scale. In Fig. 10 a small quantity of strätlingite is predicted to begin to form at approximately 250,000 h (29 years), indicating a potential for belite hydration well in excess of the 90-day experimental duration. Simulations containing gypsum appear to be more inclined to the formation of strätlingite, as shown when comparing Figs. 12 and 13. This is also highlighted in Fig. 2, which displays the strätlingite signature at 7.2° 2θ, which is not shown in XRD diffractograms of mixes that are identical other than the calcium sulfate type being anhydrite. There is, however, little difference between the consumption of ye'elimite and the generation of ettringite. Little difference is displayed between the behaviours of either clinker composition, other than the increased quantity of ye'elimite in Alipre leading to increased quantities of ettringite. The increased availability of water also appears to lead to a minor increase in the production of ettringite, as has been experienced experimentally.

4. Conclusions

The 90-day development of the hydrate assemblage for two different commercial CSA clinkers, with variable quantities of anhydrite, gypsum, and water present, has been monitored and supported by thermodynamic modelling. The shear of the mix does not seem to have had any noticeable impact upon the 7 to 90-day hydrate assemblage, indicating that the low shear method has ensured effective mixing at this scale.

Between the 7 and 90-day time period, all mixes experience some degree of further ettringite growth, after ettringite has predominantly formed prior to the 7-day measurement point. The formation of ettringite is strongly dependent upon the availability of calcium sulfate, as well as water. The difference between anhydrite and gypsum appears to have had no significant difference upon the amount of ettringite formed. More ettringite was formed within Alipre mixes, simply due to the greater quantity of ye'elimite within the clinker.

The majority of ye'elimite hydrated within all mixes, with a range of between 35% and 17% of the original ye'elimite remaining after 90 days. With the hydration of ye'elimite and the formation of ettringite, the quantity of aluminium hydroxide detected by Rietveld analysis did not increase linearly with ettringite, and accounted often for less than half the weight percentage of ettringite. Such quantities are not dissimilar to those seen in the thermodynamic simulations. This could in part be due to the occasionally amorphous structure of aluminium hydroxide being difficult to detect, or its consumption in the hydration of belite to form strätlingite.

The degree of hydration of belite within all mixes appears to be low, as also predicted in the simulations conducted. Some instances of strätlingite or C-S-H formation are displayed, but in the practical experiments, only some noticeable strätlingite is observed in gypsum mixes and aided by the increased belite quantity within Alpenat clinker. Belite hydration also increases with a decreasing presence of ettringite. Some minor belite hydration is shown to be possible in the distant future by means of thermodynamic simulation, however this only indicates a potential for further hydration past 90 days. Further hydration of belite over time may lead to further strength development, but longer-term practical studies should be carried out to verify this.

Other than gypsum appearing to increase the potential for strätlingite formation, little difference has been shown between the choice of calcium sulfates. A significant quantity of both remain at 90 days in solid products containing 35% addition levels, with as much as 20% of the product being identified as unreacted anhydrite as a maximum.

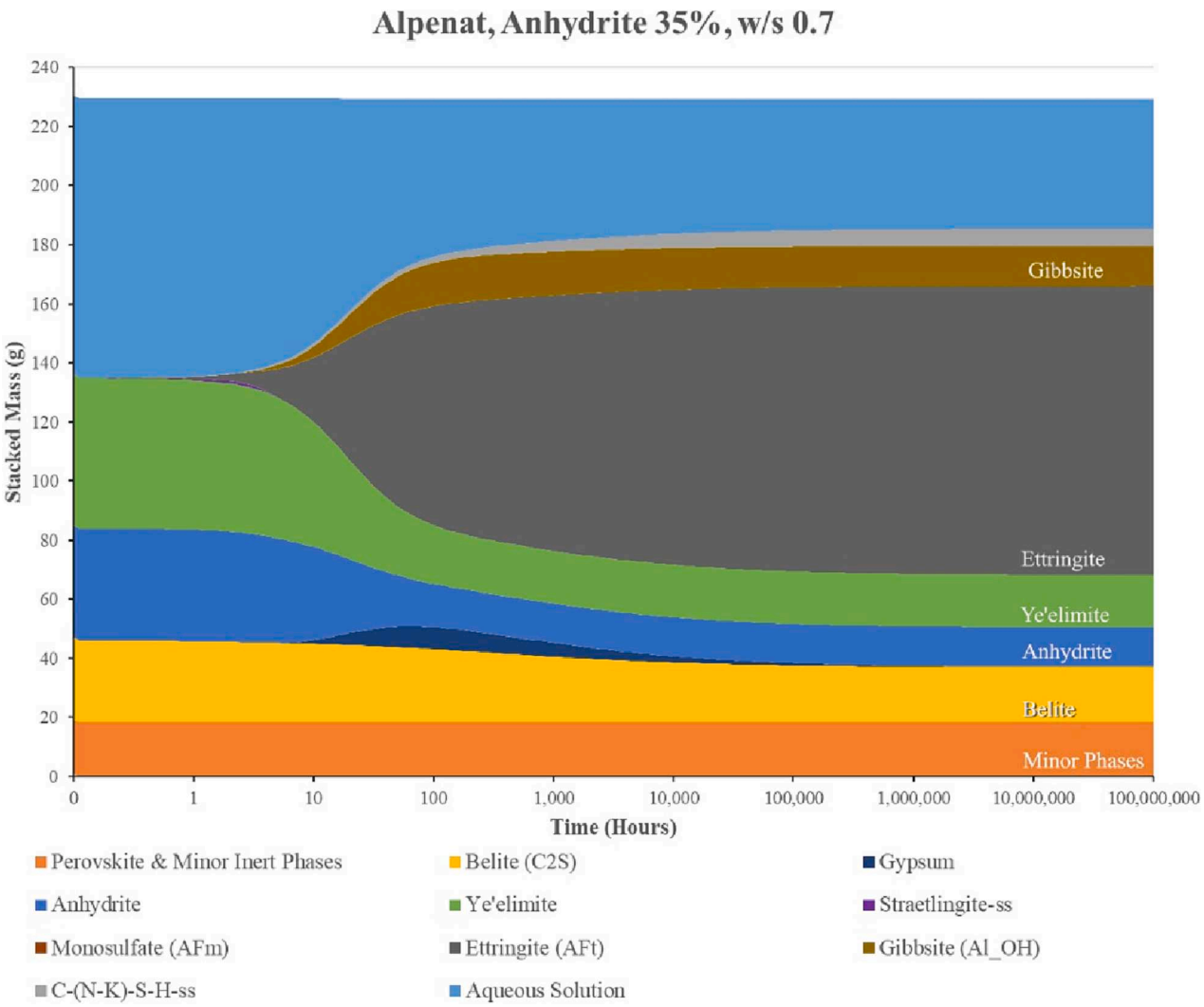

Fig. 13. CemGEMS simulation for Alpenat clinker at an anhydrite addition of 35% and a w/s ratio of 0.7. The level of hydration, so as to be comparative to experimental results, was set to 65%. The formation of strätlingite appears to benefit from the presence of gypsum over anhydrite, as development of strätlingite is negligible, with only a small quantity of C-S-H. The simulation does not identify any calcium hydroxide.

In all mixes, there is no evidence to suggest ettringite instability within the 90-day time frame studied. Within these samples cured at 20 °C and >90% RH, ettringite has only increased over time, with levels of monosulfate remaining stable, and no other mechanisms for decomposition established. Ettringite crystal size and distribution are consistent throughout this aging period and between mixes. The structure can be clearly defined using EDS mapping, with large ettringite crystals clearly distinguishable amongst the aluminium hydroxide matrix.

The predominant ettringite and aluminium hydroxide structure remains consistent throughout the varying system parameters and age under the curing conditions studied and has not broken convention at the extremities of this extensive mix formulation envelope, nor has it behaved uncharacteristically from what is expected given the variables. Both clinkers, and sources of calcium sulfate, have formed very similar phase assemblages. The calcium sulfoaluminate system therefore looks to be a robust and promising avenue for future research into the encapsulation and immobilisation of radioactive wasteforms. A scaling up of experimentation towards the 500 L practised within the nuclear industry, as well as a more complete understanding of the long-term reactivity of belite within this system and its effect upon the pore solution pH if C-S-H were to be generated, would allow for even greater confidence in CSA-belite as a potential encapsulant for radioactive waste.

CRediT authorship contribution statement

Shaun Nelson: Methodology, Investigation, Formal analysis, Data curation, Writing – original draft, Visualization. **Daniel A. Geddes:** Methodology, Investigation, Resources, Writing – review & editing. **Sarah A. Kearney:** Methodology, Investigation, Formal analysis, Writing – review & editing. **Sally Cockburn:** Investigation, Resources, Data curation, Writing – review & editing. **Martin Hayes:** Conceptualization, Methodology, Validation, Writing – review & editing, Supervision, Project administration. **Michael J. Angus:** Conceptualization, Methodology, Validation, Writing – review & editing, Supervision. **Gavin Cann:** Conceptualization, Methodology, Writing – review & editing. **John L. Provis:** Conceptualization, Methodology, Writing – review & editing, Supervision, Project administration.

Declaration of Competing Interest

The authors declare the following financial interests/personal relationships which may be considered as potential competing interests: Shaun Nelson reports financial support was provided by Engineering and Physical Sciences Research Council and the Nuclear Decommissioning Authority. All authors report financial support was provided by Sellafield Ltd.

Data availability

Data will be made available on request.

Acknowledgements

Funding for this work was provided by Sellafield Ltd and supported by the Nuclear Decommissioning Authority iCASE scheme, including partial studentship funding through this scheme from the Engineering and Physical Sciences Research Council (UK).

References

[1] Q. Zhou, N.B. Milestone, M. Hayes, An alternative to Portland cement for waste encapsulation -the calcium sulfoaluminate cement system, J. Hazard. Mater. 136 (1) (2006) 120–129, https://doi.org/10.1016/j.jhazmat.2005.11.038.
[2] S. Galluccio, T. Beirau, H. Pöllmann, Maximization of the reuse of industrial residues for the production of eco-friendly CSA-belite clinker, Constr. Build. Mater. 208 (2019) 250–257, https://doi.org/10.1016/j.conbuildmat.2019.02.148.
[3] M. García Maté, Processing and characterisation of calcium sulphoaluminate (CSA) eco-cements with tailored performances, PhD thesis, Departamento Química Inorgánica, Cristalografía, Mineralogía, Universidad de Málaga, 2014.
[4] T. Harrison, M. R. Jones, D. Lawrence, The production of low energy cements, in: *Lea's Chemistry of Cement and Concrete*, 5th ed., 2019, pp. 341-362.
[5] E.P. Bescher, Calcium Sulfoaluminate-Belite Concrete: Structure, Properties, Practice, Presented at UCLA, Los Angeles, 2018.
[6] E. Bescher, J. Kim, Belitic calcium sulfoaluminate cement: history, chemistry, performance, and use in the United States, in: 1st International Conference on Innovation in Low-Carbon, Cement & Concrete Technology (2019).
[7] J. Dachtar, Calcium Sulfoaluminate Cement as Binder for Structural Concrete., PhD thesis,, Department of Civil and Structural Engineering, The University of Sheffield, Sheffield, 2004.
[8] C.W. Hargis, A.P. Kirchheim, P.J.M. Monteiro, E.M. Gartner, Early age hydration of calcium sulfoaluminate (synthetic ye'elimite) in the presence of gypsum and varying amounts of calcium hydroxide, Cem. Concr. Res. 48 (2013) 105–115, https://doi.org/10.1016/j.cemconres.2013.03.001.
[9] Nuclear Decommissioning Authority. "How do we manage radioactive waste?" https://ukinventory.nda.gov.uk/about-radioactive-waste/how-do-we-manage-radioactive-waste/ (accessed 20/01/2022).
[10] M. J. Angus, I. H. Godfrey, M. Hayes, S. Foster, Managing change in the supply of cement powders for radioactive waste encapsulation – Twenty years of operational experience, in: Waste Management Symposium, Phoenix, Arizona, 2010.
[11] U.K. Department for Business, Energy, and Industrial Strategy. Implementing the end of unabated coal by 2025, 2018. [Online]. Available: https://assets.publishing.service.gov.uk/government/uploads/system/uploads/attachment_data/file/672137/Government_Response_to_unabated_coal_consultation_and_statement_of_policy.pdf.
[12] A. Atteridge, C. Strambo, Decline of the United Kingdom's steel industry, in: Lessons from industrial transitions, Stockholm Environment Institute, 2021.
[13] I. Bolaños-Vásquez, R. Trauchessec, J.I. Tobón, A. Lecomte, Influence of the ye'elimite/anhydrite ratio on PC-CSA hybrid cements, Mater. Today Commun. 22 (2020) 100778, https://doi.org/10.1016/j.mtcomm.2019.100778.
[14] E. Gartner, What are BYF cements, and how do they differ from CSA cements?, in: *The Future of Cement, 200 years after Louis Vicat,* pp. 6-8, 2017. Available: http://www.ecobinder-project.eu.
[15] M.L.D. Gougar, B.E. Scheetz, D.M. Roy, Ettringite and C-S-H Portland cement phases for waste ion immobilisation: A review, Waste Manag. 16 (4) (1996) 295–303.
[16] S.A. Saslow, et al., Immobilizing pertechnetate in ettringite via sulfate substitution, Environ. Sci. Tech. 54 (21) (2020) 13610–13618, https://doi.org/10.1021/acs.est.0c03119.
[17] A. Jiménez, M. Prieto, Thermal stability of ettringite exposed to atmosphere: implications for the uptake of harmful ions by cement, Environ. Sci. Tech. 49 (13) (2015) 7957–7964, https://doi.org/10.1021/acs.est.5b00536.
[18] Y.V. Seryotkin, E.V. Sokol, S.N. Kokh, M.N. Murashko, Natural Cr^{3+}-rich ettringite: occurrence, properties, and crystal structure, Phys. Chem. Miner. 45 (3) (2017) 279–292, https://doi.org/10.1007/s00269-017-0917-y.
[19] L.G. Baquerizo, T. Matschei, K.L. Scrivener, Impact of water activity on the stability of ettringite, Cem. Concr. Res. 79 (2016) 31–44, https://doi.org/10.1016/j.cemconres.2015.07.008.
[20] Y. Shen, J. Qian, J. Chai, Y. Fan, Calcium sulphoaluminate cements made with phosphogypsum: Production issues and material properties, Cem. Concr. Compos. 48 (2014) 67–74, https://doi.org/10.1016/j.cemconcomp.2014.01.009.
[21] S. Ioannou, K. Paine, L. Reig, K. Quillin, Performance characteristics of concrete based on a ternary calcium sulfoaluminate–anhydrite–fly ash cement, Cem. Concr. Compos. 55 (2015) 196–204, https://doi.org/10.1016/j.cemconcomp.2014.08.009.
[22] Q. Zhou, F.P. Glasser, Thermal stability and decomposition mechanisms of ettringite at $< 120^{\circ}C$, Cem. Concr. Res. 31 (2001) 1333–1339.
[23] Q. Zhou, E.E. Lachowski, F.P. Glasser, Metaettringite, a decomposition product of ettringite, Cem. Concr. Res. 34 (4) (2004) 703–710, https://doi.org/10.1016/j.cemconres.2003.10.027.
[24] Y. Lou, Z. Ye, S. Wang, S. Liu, X. Cheng, Influence of synthesis methods on ettringite dehydration, J. Therm. Anal. Calorim. 135 (4) (2018) 2031–2038, https://doi.org/10.1007/s10973-018-7391-8.
[25] K. Ndiaye, M. Cyr, S. Ginestet, Durability and stability of an ettringite-based material for thermal energy storage at low temperature, Cem. Concr. Res. 99 (2017) 106–115, https://doi.org/10.1016/j.cemconres.2017.05.001.
[26] H. F. W. Taylor, Portland cement and its major constituent phases, in: *Cement Chemistry*, 1997, ch. 1, pp. 1-28.
[27] M. Hayes, O. Tuck, Calcium Sulfoaluminate cement (CSA) Polypot Studies in Support of the Encapsulants Integrated Research Team (EIRT), National Nuclear Laboratory, 2019.
[28] F. Goetz-Neunhoeffer, J. Neubauer, Refined ettringite ($Ca_6Al_2(SO_4)_3(OH)_{12}\bullet 26H_2O$) structure for quantitative X-ray diffraction analysis, Powder Diffr. 21 (1) (2006) 4–11, https://doi.org/10.1154/1.2146207.
[29] H. Saalfeld, M. Wedde, Refinement of the crystal structure of gibbsite, Al(OH)3, Z. Kristall. 139 (1–6) (1974) 129–135, https://doi.org/10.1524/zkri.1974.139.16.129.
[30] R. Allmann, Refinement of the hybrid layer structure $[Ca_2Al(OH)_6]^{+}*[^1/_2SO_4{*}3H_2O]$, J. Mineral. Geochem. (1977) 136–144.
[31] Y. Dai, J. Post, Crystal structure of hillebrandite: A natural analogue of calcium silicate hydrate (CSH) phases in Portland cement, Am. Mineral. 80 (1995).
[32] N.J. Calos, C.H.L. Kennard, A.K. Whittaker, R.L. Davis, Structure of calcium aluminate sulfate $Ca_4Al_6O_{16}S$, J. Solid State Chem. 119 (1995) 1–7.
[33] A. Kirfel, G. Will, Charge density in anhydrite, $CaSO_4$, from X-ray and neutron diffraction measurements, Acta Crystallogr. B 36 (12) (1980) 2881–2890, https://doi.org/10.1107/S0567740880010461.
[34] T. Fukami, S. Tahara, K. Nakasone, C. Yasuda, Synthesis, crystal structure, and thermal properties of $CaSO_4{\cdot}2H_2O$ single crystals, Int. J. Chem. 7 (2) (2015), https://doi.org/10.5539/ijc.v7n2p12.
[35] W.G. Mumme, R.J. Hill, G. Bushnellwye, E.R. Segnit, Rietveld crystal structure refinements, crystal chemistry and calculated powder diffraction data for the polymorphs of dicalcium silicate and related phases, Neues Jahrb. Mineral. - Abhandl. 169 (1) (1995) 35–68.
[36] H. Petch, The hydrogen positions in portlandite, $Ca(OH)_2$, as indicated by the electron distribution, Acta Crystallogr. 14 (9) (1961) 950–957, https://doi.org/10.1107/S0365110X61002771.
[37] M. Bellotto, M.C. Dalconi, S. Contessi, E. Garbin, G. Artioli, Formulation, performance, hydration and rheological behavior of 'just add water' slag -based binders. in: 1st International Conference on Innovation in Low-Carbon Cement & Concrete Technology, 2019.
[38] D.K. Smith, H.R. Leider, Low-temperature thermal expansion of LiH, MgO and CaO, J. Appl. Cryst. 1 (4) (1968) 246–249, https://doi.org/10.1107/S0021889868005418.
[39] C. Bezou, A. Nonat, J.C. Mutin, A.N. Christensen, M.S. Lehmann, Investigation of the crystal structure of γ -$CaSO_4$, $CaSO_4{\cdot}0.5H_2O$, and $CaSO_4{\cdot}0.6H_2O$ by powder diffraction methods, J. Solid State Chem. 117 (1995) 165–176.
[40] S. Sasaki, C.T. Prewitt, J.D. Bass, W.A. Schulze, Orthorhombic perovskite $CaTiO_3$ and $CdTiO_3$: structure and space group, Acta Crystallogr. C 43 (9) (1987) 1668–1674, https://doi.org/10.1107/S0108270187090620.
[41] X. Bao, et al., A new $Ca_3MgSi_2O_8$ compound and some of its thermodynamic properties, J. Solid State Chem. 255 (2017) 145–149, https://doi.org/10.1016/j.jssc.2017.08.005.
[42] I. Pajares, Á.G. De la Torre, S. Martínez-Ramírez, F. Puertas, M.-T. Blanco-Varela, M.A.G. Aranda, Quantitative analysis of mineralized white Portland clinkers: The structure of fluorellestadite, Powder Diffr. 17 (4) (2002) 281–286, https://doi.org/10.1154/1.1505045.
[43] S. Sasaki, K. Fujino, Y. Takéuchi, X-ray determination of electron-density distributions in oxides, MgO, MnO, CoO, and NiO, and atomic scattering factors of their constituent atoms, Proc. Japan Acad., Series B 55 (2) (1979) 43–48, https://doi.org/10.2183/pjab.55.43.
[44] P.B. Moore, T. Araki, The crystal structure of bredigite and the genealogy of some alkaline earth orthosilicates, Am. Mineral. 61 (1976) 74–87.
[45] R. Rinaldi, M. Sacerdoti, E. Passaglia, Strätlingite: crystal structure, chemistry, and a reexamination of its polytpye vertumnite, Eur. J. Mineral. 2 (6) (1990) 841–850, https://doi.org/10.1127/ejm/2/6/0841.
[46] K. Scrivener, R. Snellings, B. Lothenbach, A Practical Guide to Microstructural Analysis of Cementitious Materials, 1st ed., CRC Press, 2016.
[47] A. Altomare, et al., The Rietveld refinement in the EXPO Software: A powerful tool at the end of the elaborate crystal structure solution pathway, Crystals 8 (2018) 12–29.
[48] Y. Jeong, C.W. Hargis, S.-C. Chun, J. Moon, The effect of water and gypsum content on strätlingite formation in calcium sulfoaluminate-belite cement pastes, Constr. Build. Mater. 166 (2018) 712–722, https://doi.org/10.1016/j.conbuildmat.2018.01.153.
[49] I. C. Madsen, N. V. Scarlett, Quantitative phase analysis, in: *Powder Diffraction Theory and Practise*, Robert. E. Dinnebier and S. J. L. Billinge Eds., 1st ed. Cambridge UK: Royal Society of Chemistry, 2008, ch. 11, pp. 298-332.
[50] D.A. Kulik, F. Winnefeld, A. Kulik, G.D. Miron, B. Lothenbach, CemGEMS – an easy-to-use web application for thermodynamic modeling of cementitious materials, RILEM Tech. Lett. 6 (2021) 36–52, https://doi.org/10.21809/rilemtechlett.2021.140.
[51] Nuclear Decommissioning Authority, Implementing Geological Disposal, 2014. [Online]. Available: https://assets.publishing.service.gov.uk/government/uploads/system/uploads/attachment/data/file/332890/GDF/White/Paper/FINAL.pdf.
[52] C. Cau-dit-Coumes, O. Farcy, P. Antonucci, J.-B. Champenois, D. Lambertin, A. Mesbah, Design of self-dessicating binders using calcium sulfoaluminate cement:

influence of the cement composition and sulfate source, Adv. Cem. Res. 31 (2019) 178–194, https://doi.org/10.1680/jadcr.18.00100.
[53] F. Winnefeld, L.H.J. Martin, C.J. Müller, B. Lothenbach, Using gypsum to control hydration kinetics of CSA cements, Constr. Build. Mater. 155 (2017) 154–163, https://doi.org/10.1016/j.conbuildmat.2017.07.217.
[54] S. Berger, C. Cau-dit-Coumes, P. Le Bescop, D. Damidot, Influence of a thermal cycle at early age on the hydration of calcium sulphoaluminate cements with variable gypsum contents, Cem. Concr. Res. 41 (2) (2011) 149–160, https://doi.org/10.1016/j.cemconres.2010.10.001.
[55] A. Cuesta, A. Ayuela, M.A.G. Aranda, Belite cements and their activation, Cem. Concr. Res. 140 (2021) #106319, https://doi.org/10.1016/j.cemconres.2020.106319.
[56] M. Borštnar, N. Daneu, S. Dolenec, Phase development and hydration kinetics of belite-calcium sulfoaluminate cements at different curing temperatures, Ceram. Int. 46 (18) (2020) 29421–29428, https://doi.org/10.1016/j.ceramint.2020.05.029.
[57] M. Liu, S. Luo, L. Yang, J. Ren, Influence of water removal techniques on the composition and microstructure of hardened calcium sulfoaluminate cement pastes, Mater. Struct. 53 (4) (2020) 89, https://doi.org/10.1617/s11527-020-01527-3.
[58] J. Kaufmann, F. Winnefeld, B. Lothenbach, Stability of ettringite in CSA cement at elevated temperatures, Adv. Cem. Res. 28 (4) (2016) 251–261, https://doi.org/10.1680/jadcr.15.00029.
[59] A. G. de la Torre, D. Londono-Zuluaga, J. M. Pineda, Behavior of belite cement blended with calcium sulfoaluminate cement: an Ecocement, in: 15th International Congress on the Chemistry of Cement, Prague, 2019.
[60] F. Winnefeld, B. Lothenbach, Hydration of calcium sulfoaluminate cements — Experimental findings and thermodynamic modelling, Cem. Concr. Res. 40 (8) (2010) 1239–1247, https://doi.org/10.1016/j.cemconres.2009.08.014.
[61] M. Mrak, F. Winnefeld, B. Lothenbach, S. Dolenec, The influence of calcium sulfate content on the hydration of belite-calcium sulfoaluminate cements with different clinker phase compositions, Mater. Struct. 54 (6) (2021) 212, https://doi.org/10.1617/s11527-021-01811-w.